1   # Optimal balancing of xylem efficiency and safety explains

2   # plant vulnerability to drought

3

4   **Authors:**

5   Oskar Franklin* [1, 2], Peter Fransson [2], Florian Hofhansl [1], Jaideep Joshi* [1]

6

7   [1] International Institute for Applied Systems Analysis, Schlossplatz 1, Laxenburg A-2361, Austria

8   [2] Department of Forest Ecology and Management, Swedish University of Agricultural Sciences, Umeå SE-

9   90283, Sweden

10

11   *Corresponding authors

12

13

Summary

- In vast areas of the world, the growth of forests and vegetation is water-limited and plant survival depends on the ability to avoid catastrophic hydraulic failure. Therefore, it is remarkable that plants take high hydraulic risks by operating at water potentials (ψ) that induce partial failure of the water conduits (xylem). Here we present an eco-evolutionary optimality principle for xylem conduit design that explains this phenomenon.
- Based on the hypothesis that conductive efficiency and safety are optimally co-adapted to the environment, we derive a simple relationship between the intrinsic tolerance to negative water potential (ψ_{50}) and the environmentally dependent minimum xylem ψ.
- This relationship is constrained by a physiological tradeoff between xylem conductivity and safety, which is relatively strong at the level of individual conduits although it may be weak at the whole sapwood level. The model explains observed variation in ψ_{50} both across a large number of species, and along the xylem path in two species. The larger hydraulic safety margin in gymnosperms compared to angiosperms is explained as an adaptation to the gymnosperms' lower capacity to recover from conductivity loss.
- The constant xylem safety factor provides a powerful principle for simplifying and improving plant and vegetation models.

Keywords: xylem, hydraulic system, vessels, tracheids, optimality, adaptation, water transport, conductance

Introduction

The hydraulic properties of plants constrain their ability to grow and survive in different environments. Therefore, a solid understanding of these constraints is essential for accurate prediction of vegetation responses to droughts and other environmental changes. In stems, the primary function of the xylem is to transport water through the stem, driven by the difference in water potential between the base and the top. The conductivity of the xylem increases steeply with the conduit diameter as long as it is not hampered by cavitation, or embolism, which happens when water potential is too low (too highly negative). The sensitivity to cavitation is often measured in terms of the water potential at which conductivity is reduced by 50%, ψ_{50}. Across a large number of species, ψ_{50} is, on average, close to the minimum midday water potential (ψ_{min}) experienced by each species, implying a remarkably small

2

45   hydraulic safety margin (ψ_{50} - ψ_{min}) (Choat *et al.*, 2012). The safety margin is lower for angiosperms than

46   gymnosperms and is smallest in wet sites with high ψ_{min}. However, the reason for this apparently risky

47   strategy and its variation with climate are not yet fully understood, despite the importance for our

48   understanding of plant responses to expected climate changes and droughts (Venturas *et al.*, 2017).

49   Here we aim to explain the variation in ψ_{50} through an eco-evolutionary-optimality perspective.

50

51   Eco-evolutionary optimality (EEO) approaches have been used to model a wide range of plant traits and

52   processes (Franklin *et al.*, 2020), including plant stomatal hydraulic regulation (Hölttä *et al.*, 2011; Wolf

53   *et al.*, 2016; Anderegg *et al.*, 2018; Wang *et al.*, 2020), vascular network structure (McCulloh *et al.*, 2003;

54   Savage *et al.*, 2010; Koçillari *et al.*, 2021), and leaf hydraulic and photosynthetic traits (Deans *et al.*,

55   2020). Xylem efficiency and safety in relation to growth environment has only rarely been addressed

56   from an EEO perspective, perhaps due to a lack of consensus on the xylem costs and benefits. For

57   example (Manzoni *et al.*, 2013) used an EEO approach based on the principle that transpiration is

58   maximized, which contrasts to the assumption in most other models that transpiration is a cost (Wang

59   *et al.*, 2017). Furthermore, although a tradeoff balancing xylem conductivity (benefit) and vulnerability

60   (cost) is expected to constrain optimal xylem function, recent studies suggest that this tradeoff is weak

61   (Gleason *et al.*, 2016; Sanchez-Martinez *et al.*, 2020; Liu *et al.*, 2021). Nevertheless, such a tradeoff is

62   invoked in the EEO-based widened pipe model explaining the stem tip to base widening of conduits

63   (Koçillari *et al.*, 2021).

64

65   Here we first show that the xylem efficiency-safety tradeoff is important at the level of conduits, even

66   though it is weaker at the level of whole sapwood tissue. Then, we combine this tradeoff with an EEO

67   hypothesis which states that plants maximize the combination of xylem conductive capacity per unit

68   conduit biomass and tolerance to low ψ. Since conductivity loss is not always reversible (Anderegg *et al.*,

69   2013; Pellizzari *et al.*, 2016) we further extend the vulnerability concept to account for accumulation of

70   irreversible conductivity loss. Our first-principles EEO-based model successfully explains the globally

71   observed relationship between ψ_{50} and the environmentally dependent ψ_{min}, and how it differs between

72   angiosperms and gymnosperms.

73

Model description and results

The conduit conductivity – safety tradeoff

76   The xylem can be seen as a network of interconnected conduits (vessels or tracheids). Xylem

77   conductivity and safety (tolerance to negative water potential, ψ_{50}) depends on both the conduits

78   themselves and their interconnections, the pits and end-walls, and how the conduits are spatially

79   clustered (Lens *et al.*, 2011). The hydraulically weighted conduit diameter (*D*) is an important

80   determinant of conductivity due to the strong effect on fluid dynamics (Hacke *et al.*, 2017), which is also

81   reflected in the ubiquitous tapering of conduits with stem height which serves to minimize the increase

82   in resistance with path length (West *et al.*, 1999). Following the Hagen–Poiseuille equation, the

83   hydraulic conductivity (maximal conductive capacity, *K*) of conduits increases with the 4th power of the

84   conduit diameter (*D*):

86    $$K = c_1 \, D^4 \tag{1}$$

88   The symbol c_1 in eq. 1, and $c_2 \dots c_6$ in the further equations, denote constants that do not matter for our

89   final results.

91   Xylem safety can be described by a vulnerability function (*P*), which describes how sapwood conductivity

92   declines with negative xylem water potential ψ. Among commonly used xylem vulnerability functions,

93   the Weibull function (eq. 2) has the advantages that it always approaches 1 as $\psi \to 0$ and that its

94   parameter *a* does not vary significantly with ψ_{50} (Duursma & Choat, 2017).

96    $$P = \left(\frac{1}{2}\right)^{\left(\frac{\psi}{\psi_{50}}\right)^a} \tag{2}$$

98   In eq.2, ψ_{50} is ψ that causes 50% loss of conductivity, which is a genetically determined functional trait

99   (Lamy *et al.*, 2014; Lobo *et al.*, 2018; Pritzkow *et al.*, 2020), evolutionarily adapted to the environmental

100   conditions experienced by a species. The parameter *a* controls the shape of *P*, and was estimated based

101   on relationship between ψ_{50} and ψ_{88} for each species using the data in (Choat *et al.*, 2012) (Appendix).

102   For angiosperms mean *a*=2.48 ± 0.15 (n=153) and for gymnosperms mean *a*=5.34 ± 0.40 (n=29), where ±

103   denotes SE.

4

105   The relative importance of different underlying traits in determining ψ_{50} varies among studies and

106   species, e.g. pit features and vessel length being most important in Acer species (Lens *et al.*, 2011) while

107   *D* and vessel grouping are important in other species (Scholz *et al.*, 2013; Levionnois *et al.*, 2021). Across

108   species, there is an inverse relationship between safety and *D* (eq. 3, where $d < 0$), which is strong in

109   some studies e.g. (Sperry *et al.*, 2006; Hacke *et al.*, 2015) and weaker, but significant, across multiple

110   studies combined (Hacke *et al.*, 2017). Thus, although xylem conductivity and safety are determined by

111   different traits in different species, across species *D* emerges as a reasonable proxy for conduit-level

112   conductivity and safety. From an eco-evolutionary standpoint, a coordination between *D* and other

113   xylem traits should be expected in order to avoid inefficiencies and bottlenecks in the conductive system

114   as a whole. Furthermore, *D* is not only linked to xylem conductivity and safety, but also influences

115   conduit wall thickness and the construction cost of conduits, which all together suggests that *D* should

116   be subject to a strong selection pressure (Koçillari *et al.*, 2021).

117

118    $\psi_{50} = -c_2\, D^d$ (3)

119

120   We estimated *d* in eq. 3 based on the data in (Sperry *et al.*, 2006) using linear regression of $\ln(\psi_{50})$

121   versus $\ln(D)$. For angiosperms $d = -1.20 \pm 0.14$, $r^2 = 0.72$ (n=29) and for gymnosperms $d = -1.32 \pm 0.63$, $r^2 =$

122   0.39 (n=18). Although other datasets may yield slightly different values of *d*, e.g. mean $d = -0.77$ in

123   angiosperms for (Hacke *et al.*, 2017), this would only have minor quantitative effects on the results as

124   long as $d < 0$.

125

126   Because both *K* and ψ_{50} depend on *D*, eqs. 1 and 3 can be combined into eq. 4, which represents a

127   conduit-level tradeoff between conductive capacity (*K*) and safety (ψ_{50}).

128

129 $K = -c_3\, \psi_{50}^{4/d}$ (4)

130

131   This tradeoff (eq. 4) is defined at the level of conductive tissue (or equivalently, probabilistically at the

132   individual-conduit level) rather than for whole-sapwood tissue. We emphasize that whole-sapwood

133   conductance also depends on the number of conduits per unit sapwood area which weakens this

134   tradeoff at the whole-plant level (Fig. 1).

135

136
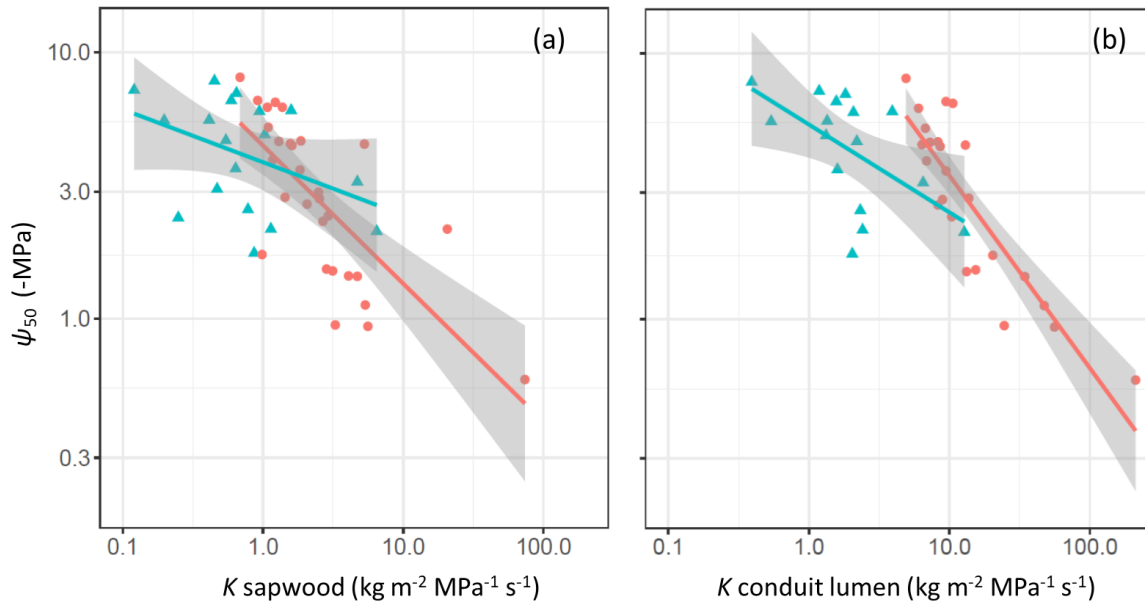
Fig. 1 Tradeoff between xylem tolerance to negative water potential (ψ_{50}) and maximal conductive capacity (K). Panels show measurements for whole sapwood (a) and for conduits only (b). Points show observations of angiosperms (red circles) and gymnosperms (blue triangles) and lines show SMA regressions with SE bands, where r^2= 0.54, 0.16 for sapwood (a) and r^2= 0.76, 0.32 for conduits (b), for angiosperms (n=29) and gymnosperms (n=18), respectively. Data from (Sperry *et al.*, 2006).

Measured vulnerability curves represent the instantaneous loss of conductivity (cavitation) but do not say anything about its reversibility and long-term costs. Conductivity losses are not always reversible (Anderegg *et al.*, 2013; Pellizzari *et al.*, 2016), which means that consecutive loss events multiply. In this case the total remaining conductivity (P_t) can be described as:

$$P_t = P \cdot P \cdot \ldots = P^i \tag{5}$$

In eq 5, *i* determines the degree of loss accumulation (irreversibility). If *i*= 1, there is no accumulation of effects; If *i*= 2, the fitness-costs of the accumulated loss of conductivity is equal in magnitude to the short-term effects; If *i* > 2, the accumulated (long-term) effects are larger than the instantaneous effects.

156 Optimal adaptation of conduit efficiency and safety

157 The higher the conductance of water through the xylem, the larger the stomatal conductance and

158 carbon uptake can be. Thus, everything else being equal, higher xylem conductance increases fitness.

159 Further, to make the most of acquired resources, all plant organs should be constructed with maximal

160 efficiency, i.e., their function (or fitness contribution) per resources invested should be maximized. The

161 benefit of the xylem is water transport and the costs accrue from the structural investment in fibers and

162 lignified tissues required to build xylem walls (Sperry, 2003). Thus, optimal xylem conduits should have a

163 high conductivity (K) per unit mass (M), i.e. conductive efficiency (K/M).

164

165 Conduit mass depends on diameter, wall thickness (T), and wall tissue density (ρ). Biophysical

166 considerations, supported by empirical observations (Hacke *et al.*, 2001; Sperry *et al.*, 2006), indicate

167 that for conduit walls to withstand negative pressure without imploding, the ratio of conduit wall

168 thickness to conduit diameter (T/D) scale with ψ_{50} according to eq.6 (Hacke *et al.*, 2001).

169

170 $\psi_{50} = -c_4\,(T/D)^2$ (6)

171

172 The mass per unit length of a conduit (M, eq. 7) can be approximated (by neglecting the difference

173 between outer and inner conduit diameter) by $\pi \cdot D \cdot T \cdot \rho$ and be expressed in terms of ψ_{50} using eqs. 6

174 and 3. The approximation introduces only a minor error in optimal ψ_{50} at highly negative values of ψ_{min}

175 (1.5% at ψ_{min} -10 MPa).

176

177 $M = \pi\,D\,T\,\rho = -c_5\,\psi_{50}^{1/2+2/d}$ (7)

178

179 In addition to having a high conductivity per mass, optimal conduits should tolerate low ψ with minimal

180 risk of conductivity loss (cavitation), i.e. P (eq. 2) should be as large as possible at the minimum

181 operating water potential (ψ_{min}, the lowest ψ measured for a given site and species). Since ψ_{min} reflects

182 the integrated effect of water flux constraints due to environmental factors and plant stomatal

183 behaviour, it exerts a strong selective force on the xylem (Bhaskar & Ackerly, 2006). Combining the two

184 criteria for optimal xylem function - high conductive efficiency and high tolerance to low ψ – in the most

185 parsimonious way, we obtain the optimality criterion, or fitness proxy, $F = \frac{K}{M} \cdot P_t(\psi = \psi_{min})$. Based on

186 eqs. 2, 4, 5 and 7, F can be expressed as a function of ψ_{50} (eq.8).

187

188 $$F = \frac{K}{M}\, P_t = -c_6\, \psi_{50}^{\frac{2}{d}-\frac{1}{2}} \left(\frac{1}{2}\right)^{i\left(\frac{\psi_{min}}{\psi_{50}}\right)^a}$$ (8)

189

190

191 The optimal ψ_{50} results from the tradeoff between increased conductive capacity per unit conduit

192 biomass and increased vulnerability with increasing ψ_{50} (Supplementary Fig. S1). F is maximized when dF

193 /dψ_{50} = 0, which results in an optimal ψ^*_{50} that is proportional to ψ_{min} (eq. 9, derivation in Appendix).

194 $$\psi^*_{50} = \psi_{min} \left(\frac{2\,a\ln(2)\,i\,d}{d-4}\right)^{\frac{1}{a}}$$ (9)

195

196 In agreement with observations, eq. 9 implies a linear relationship between ψ_{min} and ψ_{50} with zero

197 intercept, i.e. a constant ratio, or safety factor ψ_{50}/ψ_{min} (Fig. 2). For angiosperms, the observed mean

198 safety factor (0.92) is almost identical to the predicted (0.91) for the model without accumulation of

199 conductivity losses (i= 1). For gymnosperms, the observed safety factor is 1.7, which can be explained by

200 the model with conductivity loss accumulation ($i \neq 1$). For this model, i was estimated based on the

201 observations, resulting in i = 0.99 ± 0.057 (not significant different from 1) for angiosperms and i = 9.28 ±

202 1.94 for gymnosperms, indicating that gymnosperms are much more sensitive to conductivity loss

203 accumulation than angiosperms. The difference in i was the main explanation for the higher safety

204 factor in gymnosperms than in angiosperms, whereas the slightly steeper conductivity-safety tradeoff

205 (lower d) and the steeper slope of vulnerability function (due to larger a) explained 22% of the effect. In

206 addition to the interspecies variation, the model also explains the increase in negative ψ_{50} with ψ_{min}

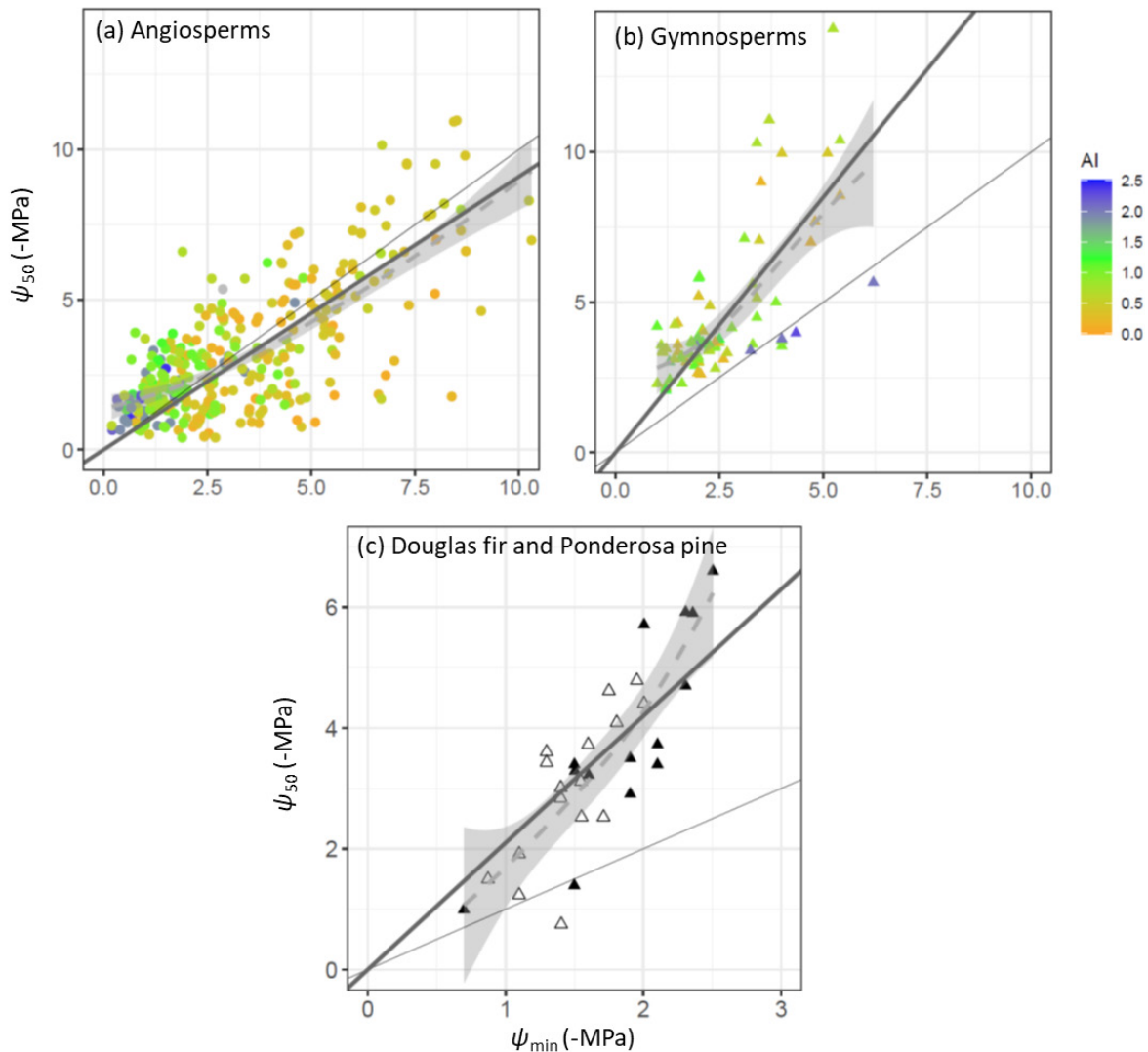207 along the hydraulic path from roots to branches in two gymnosperm species (Fig. 2c).

208

209

210

211

8

Fig. 2. Observed and modelled xylem tolerance to negative water potential (ψ_{50}) versus minimum plant water potential (ψ_{min}). (a and b) Measurements in terminal branches for different species and sites (Liu *et al.*, 2019), where colors indicate site aridity index (AI) from arid (orange) to wet (blue). Symbol shape indicates angiosperms (a, circles) and gymnosperms (b, triangles). (c) Measurements (means of 5-6 individuals) along the hydraulic path from roots, trunks and branches in Douglas fir (closed triangles) and Ponderosa pine (open triangles) (Domec *et al.*, 2009). The dashed lines with shading show smoothed mean and SE intervals of the observed relationships. The straight thick lines are the model predictions (eq. 9). The thin black line is the 1:1 line. Modeled versus observed r^2 was 0.64 for Douglas fir and Ponderosa pine (n=30), 0.51 for angiosperms (n=338), and 0.48 for gymnosperms (n = 83).

223   Importantly, the proposed optimality principle defines the intrinsic properties of conduit tissue but does

224   not determine whole sapwood or whole stem conductance. In a whole plant perspective, the principle

225   of optimal conductive efficiency operates at the lowest organizational level, i.e. the level of conduit

226   tissue. Higher-level organizational principles of xylem function are not alternative but complementary to

227   our tissue level principle. While other principles control the variation in xylem structure with plant

228   height or variation in behavioral strategies, optimal conduit efficiency and safety is always maintained at

229   the conduit level. For example, while our principle determines ψ_{50} and D at the top of stem, the widened

230   pipe model predicts the relative increase of D and decrease of ψ_{50} towards the base (Koçillari *et al.*,

231   2021).

232

Discussion

234   It was previously not explained why so many plants operate with such a small safety margin (ψ_{50} - ψ_{min}).

235   Our model explains why this is the case – it is the optimal combination of conductive capacity per

236   biomass (K/M) and tolerance to the lowest ψ experienced by a plant in its environment. The variation in

237   conductive capacity (K) relative to low ψ tolerance is constrained by an intrinsic physiological tradeoff

238   linked to conduit diameter (D). Importantly, this tradeoff is most relevant at the level of conductive

239   tissue only rather than for the whole sapwood (Fig. 1). Weak tradeoffs observed at the whole-sapwood

240   level (Gleason *et al.*, 2016) may be caused by the large variability among species in the number of

241   conduits per sapwood area (Zanne *et al.*, 2010) and the associated variation in conductivity. Although

242   vulnerability is often more strongly linked to pit- and other traits than to D within groups of similar

243   species, across a wide range of species D provides a proxy for vulnerability that allows us to link it to

244   xylem conductivity and construction costs. The relevance of optimal adaptation of D based on a

245   conductive efficiency – safety tradeoff is further supported by its success in predicting the relative tip to

246   base widening of D across species (Koçillari *et al.*, 2021).

247

248   The model further provides a theoretical explanation and quantification of the previously observed

249   general increase in the hydraulic safety margin with increasingly negative ψ_{min} (Meinzer *et al.*, 2009;

250   Choat *et al.*, 2012), which results in a constant safety factor (ψ_{50} / ψ_{min}) across species of the same type

251   (Fig. 2). Although relevant observations of variation in ψ_{min} and ψ_{50} within individuals are yet limited, the

252   available data suggest that the same optimality principle determines ψ_{50} both across different species

253   and sites and along the xylem flow path within individuals (Fig. 2).

254

255 Our simple theoretical model is limited by the few traits explicitly accounted for, not including variation

256 in capacitance, vessel grouping, and pit structure. However, because consistent data on such additional

257 traits are not widely available across species, adding more traits in the model is unlikely to improve its

258 performance, already explaining 50% of the variation in ψ_{50} across species. Whereas the model captures

259 well the overall trends in ψ_{50}, ψ_{50} for less negative ψ_{min} (wet sites) is more negative than predicted by

260 the model (Fig. 2a, b). This bias could be related to an under-estimation of negative ψ_{min} at wetter sites

261 owing to lower sampling of rare dry days at such sites compared to more frequently occurring dry days

262 at drier sites. Plants at wetter sites may be adapted to infrequent drought events which may be missed

263 in the sampling of ψ_{min} (Martinez Vilalta *et al.*, 2021).

264

265 The model accurately predicts the observed mean safety factor ψ_{50}/ψ_{min} = 0.92 in angiosperms, without

266 including irreversible or accumulating loss of conductivity. This may be related to the ability of

267 angiosperms to actively reverse embolism due to the presence of sieve tubes and companion cells in

268 their parenchyma (Johnson *et al.*, 2012; Kiorapostolou *et al.*, 2019). The much higher mean safety factor

269 in gymnosperm ψ_{50}/ψ_{min}= 1.7 indicates an adaptation to accumulating effects of conductivity loss and a

270 low reversal capacity (high *i*). A negative relationship between safety factor and embolism reversal

271 capacity is supported by previous observations (Ogasa *et al.*, 2013). The importance of irreversible

272 effects of conductivity loss for gymnosperms is further supported by the observations of a low lethal

273 negative ψ close to ψ_{50} (Liang *et al.*, 2021).

274

275 The invariant ψ_{50}/ψ_{min} ratio predicted by our theory suggests that the presence of larger conduit

276 diameters in taller plants (Olson *et al.*, 2018) does not necessarily mean that they operate at a higher

277 risk compared to shorter plants. Rather, our hypothesis suggests that taller plants with higher ψ_{50} should

278 also have higher ψ_{min} than shorter plants, which is in agreement with observations across a large

279 number of species and environments (Liu *et al.*, 2019). In a growing tree with increasing conduit

280 diameter, optimal ψ_{50}/ψ_{min} ratio could be maintained by increasing whole xylem conductivity through

281 additional conduits, more conservative stomatal regulation, or by means of increased water uptake with

282 deeper roots, i.e. drought avoidance (Brum *et al.*, 2017; Oliveira *et al.*, 2021). Nevertheless, if these

283 compensatory mechanisms are hampered by severe drought, taller trees would still suffer more than

284 shorter trees (Rowland *et al.*, 2015).

285

286 In conclusion, our results show that apparent risky hydraulic behavior of plants can be explained by an

287 eco-evolutionarily optimal design of xylem conduits, constrained by a strong xylem efficiency – safety

288 tradeoff at the scale of individual conduits. ψ_{50} is universally proportional to ψ_{min}, corresponding to a

289 constant mean safety factor $\psi_{50} / \psi_{min} \approx 0.9$ and 1.7 for angiosperms and gymnosperms, respectively.

290 The large safety factor in gymnosperms is likely an adaptation to their small capacity to recover from

291 loss of conductivity compared to angiosperms. The constant safety factor holds across environments

292 and species, and potentially also within individual trees, and thus provides a powerful principle for

293 simplifying and improving plant and vegetation models.

294

295

296 ## References

297 **Anderegg WRL, Plavcová L, Anderegg LDL, Hacke UG, Berry JA, Field CB. 2013.** Drought's legacy:
298   multiyear hydraulic deterioration underlies widespread aspen forest die-off and portends
299   increased future risk. *Global Change Biology* **19**(4): 1188-1196.
300 **Anderegg WRL, Wolf A, Arango-Velez A, Choat B, Chmura DJ, Jansen S, Kolb T, Li S, Meinzer FC, Pita P,**
301   **Resco de Dios V, Sperry JS, Wolfe BT, Pacala S. 2018.** Woody plants optimise stomatal
302   behaviour relative to hydraulic risk. *Ecology Letters* **21**(7): 968-977.
303 **Bhaskar R, Ackerly DD. 2006.** Ecological relevance of minimum seasonal water potentials. *Physiologia*
304   *Plantarum* **127**(3): 353-359.
305 **Brum M, Teodoro G, Abrahão A, Oliveira R. 2017.** Coordination of rooting depth and leaf hydraulic
306   traits defines drought-related strategies in the campos rupestres, a tropical montane
307   biodiversity hotspot. *Plant and Soil* **420**: 1-14.
308 **Choat B, Jansen S, Brodribb TJ, Cochard H, Delzon S, Bhaskar R, Bucci SJ, Feild TS, Gleason SM, Hacke**
309   **UG, Jacobsen AL, Lens F, Maherali H, Martínez-Vilalta J, Mayr S, Mencuccini M, Mitchell PJ,**
310   **Nardini A, Pittermann J, Pratt RB, Sperry JS, Westoby M, Wright IJ, Zanne AE. 2012.** Global
311   convergence in the vulnerability of forests to drought. *Nature* **491**(7426): 752-755.
312 **Deans RM, Brodribb TJ, Busch FA, Farquhar GD. 2020.** Optimization can provide the fundamental link
313   between leaf photosynthesis, gas exchange and water relations. *Nature Plants* **6**(9): 1116-1125.
314 **Domec J-C, Warren JM, Meinzer FC, Lachenbruch B. 2009.** Safety Factors for Xylem Failure by Implosion
315   and Air-Seeding Within Roots, Trunks and Branches of Young and Old Conifer Trees. *IAWA*
316   *Journal* **30**(2): 101-120.
317 **Duursma RA, Choat B. 2017.** fitplc: an R package to fit hydraulic vulnerability curves. *Journal of Plant*
318   *Hydraulics* **4**: e002.
319 **Franklin O, Harrison SP, Dewar R, Farrior CE, Brännström Å, Dieckmann U, Pietsch S, Falster D, Cramer**
320   **W, Loreau M, Wang H, Mäkelä A, Rebel KT, Meron E, Schymanski SJ, Rovenskaya E, Stocker**
321   **BD, Zaehle S, Manzoni S, van Oijen M, Wright IJ, Ciais P, van Bodegom PM, Peñuelas J,**
322   **Hofhansl F, Terrer C, Soudzilovskaia NA, Midgley G, Prentice IC. 2020.** Organizing principles for
323   vegetation dynamics. *Nature Plants* **6**(5): 444-453.
324 **Gleason SM, Westoby M, Jansen S, Choat B, Hacke UG, Pratt RB, Bhaskar R, Brodribb TJ, Bucci SJ, Cao**
325   **K-F, Cochard H, Delzon S, Domec J-C, Fan Z-X, Feild TS, Jacobsen AL, Johnson DM, Lens F,**
326   **Maherali H, Martínez-Vilalta J, Mayr S, McCulloh KA, Mencuccini M, Mitchell PJ, Morris H,**

327   **Nardini A, Pittermann J, Plavcová L, Schreiber SG, Sperry JS, Wright IJ, Zanne AE. 2016.** Weak
328   tradeoff between xylem safety and xylem-specific hydraulic efficiency across the world's woody
329   plant species. *New Phytologist* **209**(1): 123-136.
330 **Hacke UG, Sperry JS, Pockman WT, Davis SD, McCulloh KA. 2001.** Trends in wood density and structure
331   are linked to prevention of xylem implosion by negative pressure. *Oecologia* **126**(4): 457-461.
332 **Hacke UG, Spicer R, Schreiber SG, Plavcová L. 2017.** An ecophysiological and developmental perspective
333   on variation in vessel diameter. *Plant, Cell & Environment* **40**(6): 831-845.
334 **Hacke UG, Venturas MD, MacKinnon ED, Jacobsen AL, Sperry JS, Pratt RB. 2015.** The standard
335   centrifuge method accurately measures vulnerability curves of long-vesselled olive stems. *New
336   Phytologist* **205**(1): 116-127.
337 **Hölttä T, Mencuccini M, Nikinmaa E. 2011.** A carbon cost–gain model explains the observed patterns of
338   xylem safety and efficiency. *Plant, Cell & Environment* **34**(11): 1819-1834.
339 **Johnson DM, McCulloh KA, Woodruff DR, Meinzer FC. 2012.** Hydraulic safety margins and embolism
340   reversal in stems and leaves: Why are conifers and angiosperms so different? *Plant Science* **195**:
341   48-53.
342 **Kiorapostolou N, Da Sois L, Petruzzellis F, Savi T, Trifilò P, Nardini A, Petit G. 2019.** Vulnerability to
343   xylem embolism correlates to wood parenchyma fraction in angiosperms but not in
344   gymnosperms. *Tree Physiology* **39**(10): 1675-1684.
345 **Koçillari L, Olson ME, Suweis S, Rocha RP, Lovison A, Cardin F, Dawson TE, Echeverría A, Fajardo A,
346   Lechthaler S, Martínez-Pérez C, Marcati CR, Chung K-F, Rosell JA, Segovia-Rivas A, Williams CB,
347   Petrone-Mendoza E, Rinaldo A, Anfodillo T, Banavar JR, Maritan A. 2021.** The Widened Pipe
348   Model of plant hydraulic evolution. *Proceedings of the National Academy of Sciences* **118**(22):
349   e2100314118.
350 **Lamy J-B, Delzon S, Bouche PS, Alia R, Vendramin GG, Cochard H, Plomion C. 2014.** Limited genetic
351   variability and phenotypic plasticity detected for cavitation resistance in a Mediterranean pine.
352   *New Phytologist* **201**(3): 874-886.
353 **Lens F, Sperry JS, Christman MA, Choat B, Rabaey D, Jansen S. 2011.** Testing hypotheses that link wood
354   anatomy to cavitation resistance and hydraulic conductivity in the genus Acer. *New Phytologist*
355   **190**(3): 709-723.
356 **Levionnois S, Jansen S, Wandji RT, Beauchêne J, Ziegler C, Coste S, Stahl C, Delzon S, Authier L, Heuret
357   P. 2021.** Linking drought-induced xylem embolism resistance to wood anatomical traits in
358   Neotropical trees. *New Phytologist* **229**(3): 1453-1466.
359 **Liang X, Ye Q, Liu H, Brodribb TJ. 2021.** Wood density predicts mortality threshold for diverse trees.
360   *New Phytologist* **229**(6): 3053-3057.
361 **Liu H, Gleason SM, Hao G, Hua L, He P, Goldstein G, Ye Q. 2019.** Hydraulic traits are coordinated with
362   maximum plant height at the global scale. *Science Advances* **5**(2): eaav1332.
363 **Liu H, Ye Q, Gleason SM, He P, Yin D. 2021.** Weak tradeoff between xylem hydraulic efficiency and
364   safety: climatic seasonality matters. *New Phytologist* **229**(3): 1440-1452.
365 **Lobo A, Torres-Ruiz JM, Burlett R, Lemaire C, Parise C, Francioni C, Truffaut L, Tomášková I, Hansen JK,
366   Kjær ED, Kremer A, Delzon S. 2018.** Assessing inter- and intraspecific variability of xylem
367   vulnerability to embolism in oaks. *Forest Ecology and Management* **424**: 53-61.
368 **Manzoni S, Vico G, Katul G, Palmroth S, Jackson RB, Porporato A. 2013.** Hydraulic limits on maximum
369   plant transpiration and the emergence of the safety–efficiency trade-off. *New Phytologist*
370   **198**(1): 169-178.
371 **Martinez Vilalta J, Santiago L, Poyatos R, Badiella L, De Cáceres M, Aranda I, Delzon S, Vilagrosa A,
372   Mencuccini M. 2021.** Towards a statistically robust determination of minimum water potential
373   and hydraulic risk in plants. *New Phytologist* **232**(1): 404-417.

374 **McCulloh KA, Sperry JS, Adler FR. 2003.** Water transport in plants obeys Murray's law. *Nature*
375   **421**(6926): 939-942.
376 **Meinzer FC, Johnson DM, Lachenbruch B, McCulloh KA, Woodruff DR. 2009.** Xylem hydraulic safety
377   margins in woody plants: coordination of stomatal control of xylem tension with hydraulic
378   capacitance. *Functional Ecology* **23**(5): 922-930.
379 **Ogasa M, Miki NH, Murakami Y, Yoshikawa K. 2013.** Recovery performance in xylem hydraulic
380   conductivity is correlated with cavitation resistance for temperate deciduous tree species. *Tree*
381   *Physiology* **33**(4): 335-344.
382 **Oliveira RS, Eller CB, Barros FdV, Hirota M, Brum M, Bittencourt P. 2021.** Linking plant hydraulics and
383   the fast–slow continuum to understand resilience to drought in tropical ecosystems. *New*
384   *Phytologist* **230**(3): 904-923.
385 **Olson ME, Soriano D, Rosell JA, Anfodillo T, Donoghue MJ, Edwards EJ, León-Gómez C, Dawson T,**
386   **Camarero Martínez JJ, Castorena M, Echeverría A, Espinosa CI, Fajardo A, Gazol A, Isnard S,**
387   **Lima RS, Marcati CR, Méndez-Alonzo R. 2018.** Plant height and hydraulic vulnerability to
388   drought and cold. *Proceedings of the National Academy of Sciences* **115**(29): 7551-7556.
389 **Pellizzari E, Camarero JJ, Gazol A, Sangüesa-Barreda G, Carrer M. 2016.** Wood anatomy and carbon-
390   isotope discrimination support long-term hydraulic deterioration as a major cause of drought-
391   induced dieback. *Global Change Biology* **22**(6): 2125-2137.
392 **Pritzkow C, Williamson V, Szota C, Trouvé R, Arndt SK. 2020.** Phenotypic plasticity and genetic
393   adaptation of functional traits influences intra-specific variation in hydraulic efficiency and
394   safety. *Tree Physiology* **40**(2): 215-229.
395 **Rowland L, da Costa ACL, Galbraith DR, Oliveira RS, Binks OJ, Oliveira AAR, Pullen AM, Doughty CE,**
396   **Metcalfe DB, Vasconcelos SS, Ferreira LV, Malhi Y, Grace J, Mencuccini M, Meir P. 2015.** Death
397   from drought in tropical forests is triggered by hydraulics not carbon starvation. *Nature*
398   **528**(7580): 119-122.
399 **Sanchez-Martinez P, Martínez-Vilalta J, Dexter KG, Segovia RA, Mencuccini M. 2020.** Adaptation and
400   coordinated evolution of plant hydraulic traits. *Ecology Letters* **23**(11): 1599-1610.
401 **Savage VM, Bentley LP, Enquist BJ, Sperry JS, Smith DD, Reich PB, Von Allmen EI. 2010.** Hydraulic
402   trade-offs and space filling enable better predictions of vascular structure and function in plants.
403   *Proceedings of the National Academy of Sciences of the United States of America* **107**(52):
404   22722-22727.
405 **Scholz A, Rabaey D, Stein A, Cochard H, Smets E, Jansen S. 2013.** The evolution and function of vessel
406   and pit characters with respect to cavitation resistance across 10 Prunus species. *Tree*
407   *Physiology* **33**(7): 684-694.
408 **Sperry JS. 2003.** Evolution of Water Transport and Xylem Structure. *International Journal of Plant*
409   *Sciences* **164**(S3): 115-127.
410 **Sperry JS, Hacke UG, Pittermann J. 2006.** Size and function in conifer tracheids and angiosperm vessels.
411   *American Journal of Botany* **93**(10): 1490-1500.
412 **Venturas MD, Sperry JS, Hacke UG. 2017.** Plant xylem hydraulics: What we understand, current
413   research, and future challenges. *Journal of Integrative Plant Biology* **59**(6): 356-389.
414 **Wang H, Prentice IC, Keenan TF, Davis TW, Wright IJ, Cornwell WK, Evans BJ, Peng C. 2017.** Towards a
415   universal model for carbon dioxide uptake by plants. *Nature Plants* **3**(9): 734-741.
416 **Wang Y, Sperry JS, Anderegg WRL, Venturas MD, Trugman AT. 2020.** A theoretical and empirical
417   assessment of stomatal optimization modeling. *New Phytologist* **227**(2): 311-325.
418 **West GB, Brown JH, Enquist BJ. 1999.** A general model for the structure and allometry of plant vascular
419   systems. *Nature* **400**(6745): 664-667.

420   **Wolf A, Anderegg WRL, Pacala SW. 2016.** Optimal stomatal behavior with competition for water and
421   risk of hydraulic impairment. *Proceedings of the National Academy of Sciences* **113**(46): E7222-
422   E7230.

423   **Zanne AE, Westoby M, Falster DS, Ackerly DD, Loarie SR, Arnold SEJ, Coomes DA. 2010.** Angiosperm
424   wood structure: Global patterns in vessel anatomy and their relation to wood density and
425   potential conductivity. *American Journal of Botany* **97**(2): 207-215.

426
427

Acknowledgements

Author contributions

O.F. conceived the original idea, analyzed the data, and wrote the draft manuscript. J.J. and P.F. contributed complementary mathematical analyses. F.H. and J.J. provided complementary data. All authors contributed to conceptual development and the final manuscript.

439 # Appendix

440 ## Mathematical derivations

441 ### Derivation of optimal ψ_{50}

442 The combined conductive efficiency and safety (F) is given by eq.8, as illustrated in Fig. A1.

443 $$F = \frac{K}{M} \, P = -c_5 \, \psi_{50}^{\frac{2}{d}-\frac{1}{2}} \left(\frac{1}{2}\right)^{i \left(\frac{\psi}{\psi_{50}}\right)^a}$$

444

445 Maximization of F with respect to ψ_{50} implies that

446 $\frac{\partial F}{\partial \psi_{50}} = 0$ and that $\frac{\partial ln(F)}{\partial \psi_{50}} = 0.$

447

448 $$ln(F) = ln(c_5) + \left(\frac{2}{d} - \frac{1}{2}\right) ln(\psi_{50}) + i \left(\frac{\psi}{\psi_{50}}\right)^a ln\left(\frac{1}{2}\right)$$
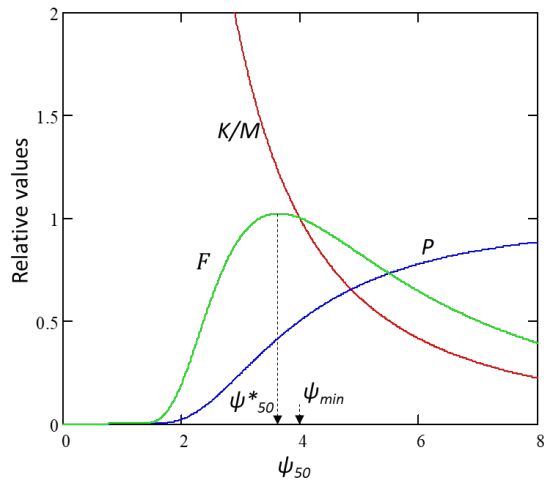
449 $\frac{\partial ln(F)}{\partial \psi_{50}} = \left(\frac{2}{d} - \frac{1}{2}\right) + i \left(\frac{\psi}{\psi_{50}}\right)^a a \ln(2) = 0$, which is solved for ψ_{50} to yield optimal ψ_{50} (ψ_{50}^*) as a function

450 of $\psi = \psi_{min}$:

451 $$\psi_{50}^* = \psi_{min} \left(\frac{2 \, a \ln(2) \, i \, d}{d-4}\right)^{\frac{1}{a}} \quad \text{(eq. 9)}$$

452

453

454
455 **Fig A1.** Optimal ψ^*_{50} resulting from maximization of $F = \frac{K}{M} \cdot P$ (eq. 8), where $\frac{K}{M}$ (red line) and F (green
456 line) are shown normalized with respect to their values at $\psi_{50} = \psi_{min}$.
457
458

459 ### Calculation of the parameter a in the vulnerability function

460 Ψ_{88} corresponds to 88% loss of conductivity, which is inserted into the vulnerability function P (eq. 2),
461 which is solved for a.

462 $$P(\psi = \psi_{88}) = 1 - 0.88 = 0.12 = \left(\frac{1}{2}\right)^{\left(\frac{\psi_{88}}{\psi_{50}}\right)^a}$$

463

17

464

$$a = \frac{\ln\left(\frac{-\ln(0.12)}{\ln(2)}\right)}{\ln\left(\frac{\ln(\psi_{88})}{\ln(\psi_{50})}\right)}$$

465